PHYSICAL REVIEW B VOLUME 60, NUMBER 20 15 NOVEMBER 1999-II

# Orbital current mode in elliptical quantum dots

Llorenç Serra and Antonio Puente
*Departament de Física, Universitat de les Illes Balears, E-07071 Palma de Mallorca, Spain*

Enrico Lipparini
*Dipartimento di Fisica, Università di Trento, I-38050 Povo, Italy*
*and INFM sezione di Trento, I-38050 Povo, Italy*

(Received 5 August 1999)

An orbital current mode peculiar to deformed quantum dots is theoretically investigated; first by using a simple model that makes it possible to analytically interpret its main characteristics, and second, by numerically solving the microscopic equations of time evolution after an initial perturbation within the time-dependent local-spin-density approximation. Results for different deformations and sizes are shown. [S0163-1829(99)50244-0]

The study of collective excitations in semiconductor quantum dots is currently attracting much interest. Recent experiments, using resonant Raman scattering in two-dimensional GaAs-$Al_xGa_{1-x}As$ quantum dots,[1,2] have probed both charge-density and spin-density collective excitations, as well as single-particle excitations. From the theoretical side, charge-density excitations have been investigated since several years ago, with different approaches, such as Hartree,[3] Hartree-Fock,[4] and density-functional theory.[5] In addition, a general scheme to describe spin-density excitations of both longitudinal and transverse character was presented in Refs. 5 and 6. All these theoretical calculations applied the well-known random-phase approximation in circularly symmetric dots, for which the angular momentum selection rules can be exploited.

Experiments on deformed nanostructures are currently providing very interesting pieces of information (for instance, in Ref. 7 on ellipsoidal deformations). This has prompted, in Refs. 8–11, the extension of theoretical approaches to the symmetry-unrestricted situation. Motivated by this exciting direction of the quantum dot field, we report in this communication on an unusual class of collective excitations. It involves the generation of orbital currents and is peculiar to deformed quantum dots. We will show that the orbital current excitation (OCE) is strongly connected to the quadrupole charge-density excitation (QCDE), and that its clearest signature is in the magnetic dipole strength (M1). The characteristics of this mode will be investigated first analytically, by using a simplified model, and second, by numerically solving the time-dependent Kohn-Sham equations corresponding to this particular motion. It is worthwhile to point out that current modes similar to this one have been measured[12] and theoretically predicted[13] in atomic nuclei, and are also expected to exist in deformed metal clusters,[14] and in the condensate of trapped bosons. In fact, while writing the present paper, we have become aware of a microscopic calculation for metal clusters, using a schematic random-phase approximation, that has been published in Ref. 15, and one for Bose gases which is in preparation.[16]

Let us assume a perfectly elliptic quantum dot, whose electron $\rho$ and kinetic energy $\tau$ densities are functions of the ellipse contour lines

$$\rho(\mathbf{r}) \equiv \rho\left(\frac{x^2}{R_x^2}+\frac{y^2}{R_y^2}\right)$$

$$\tau(\mathbf{r}) \equiv \tau\left(\frac{x^2}{R_x^2}+\frac{y^2}{R_y^2}\right), \tag{1}$$

where $R_x$ and $R_y$ are the ellipse radii. If $R_x = R_y$, we obviously recover the circularly symmetric densities. A time-dependent displacement may be represented as $\alpha(t)\mathbf{u}(\mathbf{r})$, where $\alpha(t)$ is a time-dependent parameter and $\mathbf{u}(\mathbf{r})$ gives the vector displacement at point $\mathbf{r}$. The corresponding displacement operator $\mathcal{D}$, that acting on the $N$-electron ground state gives the displaced state $|d\rangle = \mathcal{D}|0\rangle$, is

$$\mathcal{D} = \exp\left[\frac{i}{2\hbar}\alpha(t)\sum_{i=1}^{N}\left[\mathbf{u}(\mathbf{r}_i)\cdot\mathbf{p}_i + \text{H.a.}\right]\right], \tag{2}$$

where $\mathbf{p}_i$ is the $i$th electron momentum operator and H.a. stands for the Hermitian adjoint operator.

The OCE is represented by the following displacement field:

$$\mathbf{u}(\mathbf{r}) = \hat{\mathbf{e}}_z \times \mathbf{r} + \eta\nabla(xy) \equiv [-y(1-\eta), x(1+\eta)]. \tag{3}$$

It is a combination of a rigid rotation with $z$ axis and a quadrupole distortion, weighted with a parameter $\eta$. This is a divergency free field $\nabla\cdot\mathbf{u} = 0$ and, by choosing

$$\eta = \frac{R_y^2 - R_x^2}{R_x^2 + R_y^2}, \tag{4}$$

it can be shown that the density variations up to second order in $\alpha$ are

$$\delta\rho = 0 \tag{5}$$

$$\delta\tau = \frac{\alpha^2}{6}\sum_{kl}\left(\nabla_k u_l + \nabla_l u_k\right)^2\tau.$$

This result implies that the collective motion does not modify the electron density and therefore, it is not affected by the Coulomb interaction. In fact, the cost in the Coulomb

 

energy is minimized by adding the quadrupole term $\nabla(xy)$ in the displacement field (3). The collective motion associated with this field modifies the kinetic energy density and thus it is an example of an elastic (or shear) mode exhibited by a Fermi system, that has been extensively studied in atomic nuclei.[13] The electronic motion is in fact a collective rotating flow along the ellipse contour lines.

The frequency of the OCE may be estimated assuming the oscillator formula $\omega_{\rm OCE}=\sqrt{k/M}$, where the restoring force $k=2E(\mathbf{u})$ is fixed by the energy change $E(\mathbf{u})$ associated with the displacement field (3), $M=m\int \mathbf{u}^2\rho d\mathbf{r}$ is the collective mass parameter and $m$ is the single-electron effective mass. One gets

$$k=\frac{16}{3}\eta^2 E^{(0)}_{\rm kin}$$

$$M=Nm\langle r^2\rangle(1-\eta^2), \tag{6}$$

where $E^{(0)}_{\rm kin}$ is the unperturbed kinetic energy. If we further assume $\langle r^2\rangle=\frac{1}{2}r_s^2N$ and $E^{(0)}_{\rm kin}=\frac{1}{2}\varepsilon_F N$ (where $\varepsilon_F$ and $r_s$ are the Fermi energy and the Wigner-Seitz radius, respectively) we finally get

$$\omega_{\rm OCE}\approx\sqrt{\frac{16}{3}}\frac{\hbar}{mr_s^2}\frac{\eta}{\sqrt{1-\eta^2}}N^{-1/2}. \tag{7}$$

This simple expression tells us how the electronic OCE scales with $N$, deformation of the ellipse $\eta$, and electronic density ($r_s$ parameter).

Repeating a similar treatment with a pure quadrupole displacement $\mathbf{u}=\nabla(xy)$, the frequency of the QCDE can be estimated

$$\omega_{\rm QCDE}\approx\sqrt{2}\omega_0, \tag{8}$$

where $\omega_0$ is the average parameter of the external confining potentials in $x$ and $y$ directions, assumed of parabolic type, i.e., $\omega_0=(\omega_x+\omega_y)/2$ (see below).

From a physical point of view, we expect both modes, OCE and QCDE, to manifest themselves in the response to the magnetic orbital dipole (M1) operator $\mu_B L_z$, and to the electric quadrupole (E2) operator $xy$. However, to really ascertain what is the relative weight of each mode in these channels, we need to perform a more microscopic calculation. This is our goal in what follows.

We will describe the time evolution within density functional theory, in the local spin-density approximation. The time-dependent Kohn-Sham equations are solved by discretizing the $xy$ plane in a uniform grid of equally spaced points and using the Crank-Nicholson approximation. Of course, the unperturbed state is the Kohn-Sham ground state, numerically obtained by solving the static Kohn-Sham equations in the same grid by a steepest descent method. Technical details of the method can be found in Ref. 10.

The set of single-particle orbitals $\{\varphi_i(\mathbf{r})\}$ evolves in time as[17]

$$i\frac{\partial}{\partial t}\varphi_{i\eta}(\mathbf{r},t)=h_\eta[\rho,m]\,\varphi_{i\eta}(\mathbf{r},t), \tag{9}$$

where the spin index is $\eta=\uparrow,\downarrow$, and total density and magnetization are given in terms of the spin densities $\rho_\eta(\mathbf{r})=\Sigma_i|\varphi_{i\eta}(\mathbf{r})|^2$, by $\rho=\rho_\uparrow+\rho_\downarrow$ and $m=\rho_\uparrow-\rho_\downarrow$, respectively. The Hamiltonian $h_\eta$ in Eq. (9) contains, besides the kinetic energy, the confining potential $v^{(\rm conf)}(\mathbf{r})$, the Hartree potential $v^{(H)}(\mathbf{r})=\int d\mathbf{r}'\rho(\mathbf{r}')/|\mathbf{r}-\mathbf{r}'|$, and the exchange-correlation piece $v^{(xc)}_\eta(\mathbf{r})=(\partial/\partial\rho_\eta)\mathcal{E}_{xc}(\rho,m)$. The exchange-correlation energy density $\mathcal{E}_{xc}(\rho,m)$ has been described as in Refs. 8–10.

To model the elliptic quantum dots, we will follow the prescription of Refs. 7 and 9 and consider the confinement produced by anisotropic parabolas with parameters $\omega_x$ and $\omega_y$ in $x$ and $y$ directions, respectively. We define the ratio $\beta=\omega_y/\omega_x$ and fix the centroid with the Wigner-Seitz radius as $\omega_0^2=1/r_s^3\sqrt{N}$. In terms of these parameters, the external confining potential reads

$$v^{(\rm conf)}(\mathbf{r})=\frac{1}{2}\omega_0^2\frac{4}{(1+\beta)^2}(x^2+\beta^2y^2). \tag{10}$$

As discussed in Ref. 7, this is a reasonable approximation to the real confining potential in vertical quantum dots with rectangular (mesa) structure.

An initial perturbation, modeling the interaction with the physical probe, is needed in order to excite the system and monitor its time evolution. This is achieved by modifying the orbitals with the displacement operator (2). With our previous discussion, three natural options for the displacement field $\mathbf{u}(\mathbf{r})$ come inmediately to mind: a pure rotation (twist), a pure quadrupole distortion, and the combination given in

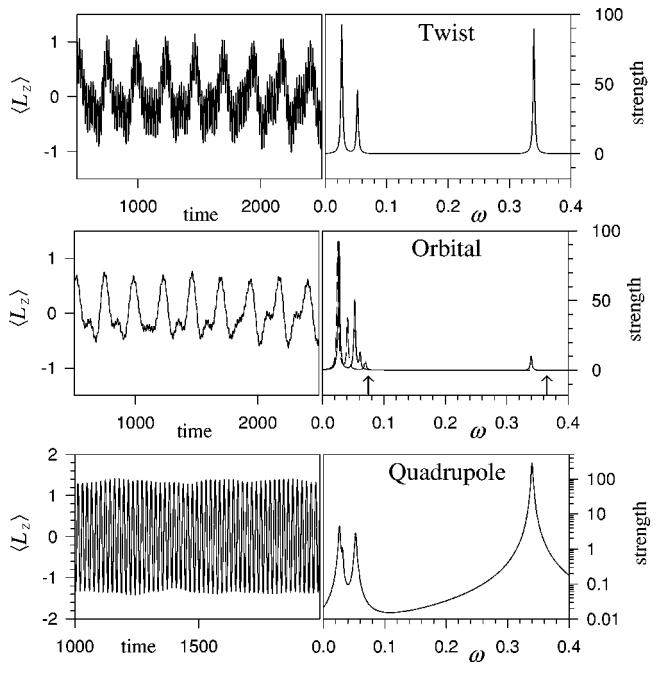


FIG. 1. Results for the time evolution of an elliptic dot with $N=20$, $\beta=0.75$, and $r_s=1.51a_0^*$, with the three different initial perturbations (rigid twist, orbital, and quadrupole distortions). Left panels display the simulated orbital M1 signal as a function of time, while right panels show the corresponding strength functions in arbitrary units. The middle right panel also shows the independent particle strength function (dashed line) and the position of the analytical approximations (7) and (8) with arrows.

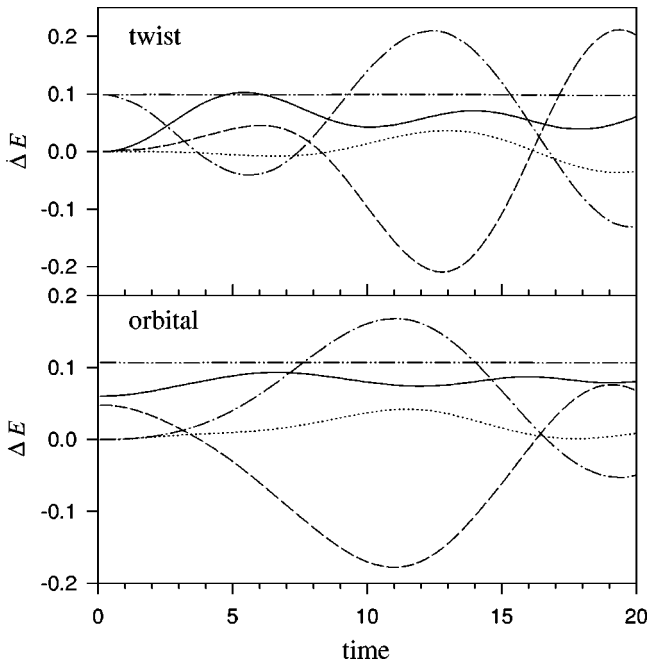


FIG. 2. Time dependence of the different energy variations after an initial twist and orbital perturbations: kinetic (solid), internal Coulomb (dash), external confining field (dash-dot), exchange-correlation (dots), and total (dash-dot-dot). Notice that the sum of kinetic, Coulomb, external field, and exchange-correlation contributions yields the total energy increment and remains constant in time.

Eq. (3) (orbital distortion). In the latter case, we fix $\eta$ with the elliptic potential parameters by assuming that $R_x/R_y = \beta$, i.e., the ratio between $x$ and $y$ radii is given by the inverse ratio of the corresponding parabola coefficients. By looking at the density contour lines, we have checked that this assumption is well satisfied. It yields

$$\eta = \frac{1-\beta^2}{1+\beta^2}. \tag{11}$$

Figure 1 shows the results for the $N=20$ electron dot confined with $r_s = 1.51a_0^*$ and $\beta = 0.75$ (i.e., $\omega_x = 0.29$ H*, $\omega_y = 0.22$ H*). This figure nicely confirms the results anticipated with the analytical model. The orbital M1 strength is divided into two clear regions. One at high energy, which is associated with the QCDE, and one at low energy associated with the OCE. The relative weight given to both states is sensitively controlled with the parameter $\eta$. When this is forced to zero (twist), the QCDE takes a large part of the M1 strength. But when $\eta$ is taken according to the system deformation, the OCE is the dominant mode. The decoupling is not perfect, as it is in the simple model, and the short period signal of the QCDE can be clearly seen, although with much lesser amplitude than for the twist excitation. The analytical expressions (7) and (8) yield for this case the numerical values 0.066 H* and 0.36 H*, respectively, which agree quite reasonably with the microscopic result. The OCE is strongly fragmented because of Landau damping. This can be seen from Fig. 1, since the OCE overlaps with peaks associated with single-particle excitations, obtained by keeping $h_\eta$ fixed to its static value in Eq. (9). In contrast, the QCDE is moved to higher energy by the residual interaction and is not fragmented. The lower panels of Fig. 1 show the M1 signal after an initial quadrupole distortion. In this case, the QCDE is the most dominant and we have used a logarithmic vertical scale to show that the OCE intensity is around 2% of the QCDE one. We conclude from Fig. 1 that the OCE produces a clear signature in the experimental orbital M1 strength of elliptical dots.

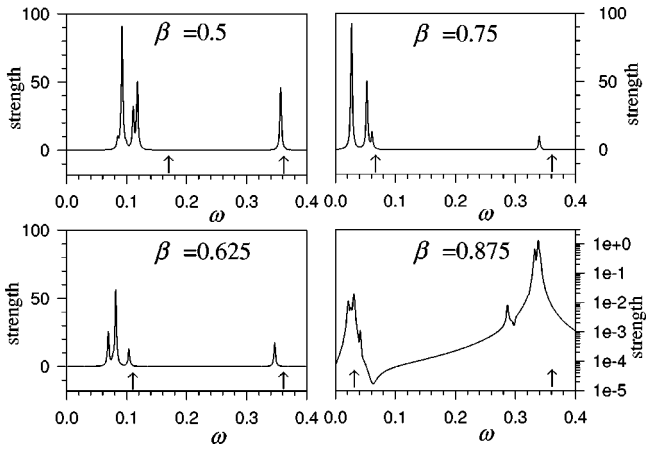


FIG. 3. Dependence of the OCE and QCDE with deformation ($\beta$ parameter, see text) for $N=20$ electrons and $r_s = 1.51a_0^*$. The arrows indicate the energies given by Eqs. (7) and (8).

We have peformed the same analysis with the $xy$ signal, corresponding to the E2 channel, with similar conclusions, although the QCDE is more dominant in this case. The fragmentation patterns are the same as for the M1 results already discussed, and the percentage of the OCE highest peak with respect to QCDE is $\sim 1\%$, $\sim 75\%$, and $\sim 1\%$ for the twist, orbital, and quadrupole distortions, respectively.

The elastic behavior of the OCE, in contrast to charge-density excitations, can be appreciated from the time evolution of the different contributions to the total energy after the initial perturbation. As seen from Fig. 2, after a rigid twist, the system only increases its energy in the external field. This triggers the motion and, as a consequence of total energy conservation, the other energy contributions begin to increase at the expense of the external field term. With per-

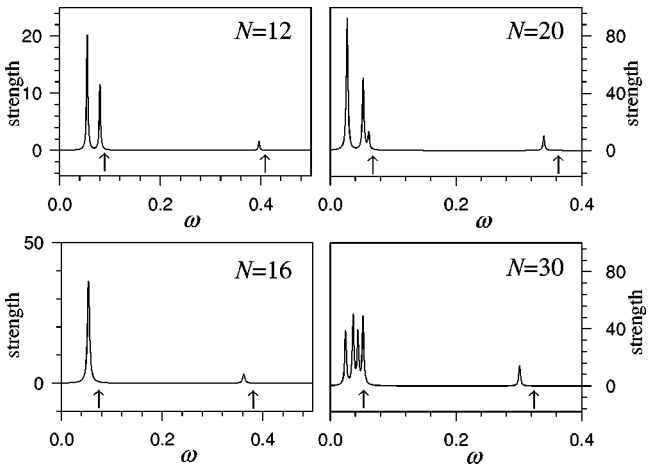


FIG. 4. Dependence with size of the OCE and QCDE strength for a fixed deformation of $\beta = 0.75$. As in Fig. 3, the arrows indicate the energies of the analytical expressions (7) and (8).

turbation (3) the situation is qualitatively different. At $t=0$, there is an important increase in both kinetic and internal Coulomb energies. The first is due to the elasticity of Fermi systems mentioned before, while the second appears because the quantal densities are not really uniform within the ellipsoid, but have shell oscillations. The rotation along the elliptic contour deforms this structure and thus increases the internal Coulomb energy. Again, because of energy conservation, once the motion has started, all contributions fluctuate in a correlated manner.

Figure 3 shows the evolution with deformation of the M1 strength, for $N=20$ and $r_s=1.51a_0^*$, after an initial orbital displacement (3). In each case, the positions of the analytical energies (7) and (8) are indicated by arrows. The energy dependence of the OCE is in qualitative agreement with Eq. (7), decreasing from $\beta=0.5$ to 0.875. However, formula (7) begins to deviate from the miscrocopic result for the highest deformation ($\beta=0.5$). The QCDE does not change much with deformation since we keep the centroid $\omega_0$ fixed. It can also be seen from this figure that when $\beta$ approaches unity, i.e., the dot becomes circular, the OCE carries less strength with respect to the QCDE. In fact, for $\beta=0.875$ we have used logarithmic scale, since the OCE height is only $\sim 1\%$ of the QCDE one.

In Fig. 4 we show the M1 strength for a fixed $\beta$ and varying the number of electrons. There is a tendency to decrease the OCE energy with increasing size, correctly pointed by the analytical expression (7). It is also seen that the fragmentation of the OCE increases with size because of the increasing role of Landau damping.

To summarize, the existence of an intense, low lying OCE in the M1 strength of elliptical quantum dots has been pointed out. The importance of this mode with respect to the QCDE, as well as its evolution with dot deformation and size, have been discussed. Our analysis is based on the time evolution of the microscopic Kohn-Sham equations and on a simplified model that allows us to obtain analytical solutions. The validity of the analytical expressions has been checked by comparison with the microscopic result. The microscopic calculation has also shown a sizeable fragmentation of this low energy mode, that we attribute to an important role of Landau damping.

This work was supported in part by Grant No. PB95-0492 from CICYT, Spain.

[1] C. Schüller *et al.*, Phys. Rev. B **54**, R17 304 (1996).
[2] R. Strenz *et al.*, Phys. Rev. Lett. **73**, 3022 (1994).
[3] D. A. Broido, K. Kempa, and P. Bakshi, Phys. Rev. B **42**, 11 400 (1990).
[4] V. Gudmundsson and R. R. Gerhardts, Phys. Rev. B **43**, 12 098 (1991); V. Gudmundsson and J. J. Palacios, *ibid.* **52**, 11 266 (1995).
[5] Ll. Serra *et al.*, Phys. Rev. B **59**, 15 290 (1999).
[6] E. Lipparini and Ll. Serra, Phys. Rev. B **57**, 6830 (1998); E. Lipparini *et al.*, *ibid.* **60**, 8734 (1999).
[7] D.G. Austing *et al.*, cond-mat/9905135 (unpublished).
[8] M. Koskinen, M. Manninen, and S. M. Reimann, Phys. Rev. B **79**, 1389 (1997).
[9] K. Hirose and N. S. Wingreen, Phys. Rev. B **59**, 4604 (1999).
[10] A. Puente and Ll. Serra, Phys. Rev. Lett. **83**, 3266 (1999); (unpublished).
[11] C. Yannouleas and U. Landman, Phys. Rev. Lett. **82**, 5325 (1999).
[12] D. Bohle *et al.*, Phys. Lett. **137B**, 27 (1984).
[13] E. Lipparini and S. Stringari, Phys. Rep. **175**, 103 (1989).
[14] E. Lipparini and S. Stringari, Phys. Rev. Lett. **63**, 570 (1989).
[15] V. O. Nesterenko *et al.*, Phys. Rev. Lett. **83**, 57 (1999).
[16] S. Stringari (private communication).
[17] We use effective atomic units corresponding to GaAs values, i.e., $H^*\approx 12$ meV, $a_0^*\approx 98$ Å, and $\tau^*\approx 55$ fs, as energy, length, and time units.